THE JOURNAL OF NAVIGATION (2004), **57**, 297–310. © The Royal Institute of Navigation
DOI: 10.1017/S037346330400267X Printed in the United Kingdom

GPS/INS Enhancement for Land Navigation using Neural Network

Burak H. Kaygisiz

(*The Scientific and Technical Research Council of Turkey*)
(Email: bkaygi@sage.tubitak.gov.tr)

Ismet Erkmen and Aydan M. Erkmen

(*Middle East Technical University*, *Turkey*)

We propose in this paper a method to enhance the performance of a coupled global positioning/inertial navigation system (GPS/INS) for land navigation applications during GPS signal loss. Our method is based on the use of an artificial neural network (ANN) to intelligently aid the GPS/INS coupled navigation system in the absence of GPS signals. The proposed enhanced GPS/INS is tested in the dynamic environment of a land vehicle navigating around a closed path on the METU campus and we provide the results. Our GPS/INS + ANN system performance is thus demonstrated with a land trial.

KEY WORDS

1. Inertial navigation. 2. Global positioning system. 3. Strapdown. 4. Neural network.

1. INTRODUCTION. Inertial Navigation (INS) and Global Positioning System (GPS) integrated navigation systems have been implemented in military applications for more than 20 years (Kaygisiz and Gokpinar, 2003). With the introduction of mass production capabilities and low cost sensors GPS/INS systems have begun to be used in civil applications such as automotive, robotics and unmanned autonomous vehicles (Kelly, 1994; Kaygisiz and Erkmen, 2003). With the impetus of technological trends and the low cost of new generation inertial sensors, one of the leading application areas of these integrated systems is land vehicle navigation. Modern autonomous and non-autonomous land vehicles designed to function in complex missions use GPS integrated with low cost INS for their navigation purposes.

The integrated navigation system yields very accurate navigation solutions provided that there is a continuous access to GPS signals (Titterton and Weston, 1997). However, a land vehicle entering a tunnel, a downtown area with high buildings, a canyon or a forest may frequently be incapable of receiving the GPS signals that are critical for the accuracy of navigation (Brown and Hwang, 1992). In the absence of GPS signals, the vehicle begins to depend solely on the low cost sensor equipped INS and will drift swiftly out of its planned trajectory so that the vehicle can be lost in the most critical part of a mission. In order to circumvent this problem, one may

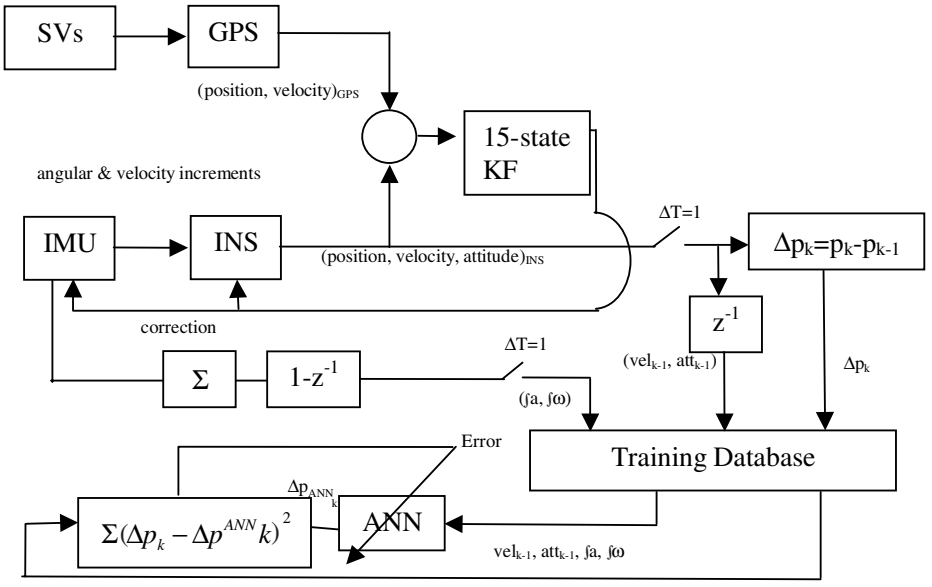

Figure 1. System block diagram (training phase).

employ higher-grade inertial sensors or additional aiding sensors other than GPS (Lewantowicz and Paschall, 1995). These approaches clearly lead to an expensive solution, which may not always be possible or desirable.

In order to handle such a problem in a cost effective manner, we propose to generate intelligent estimates of position difference based on learnt GPS/INS behaviour patterns and provide an effective intelligent support to the INS throughout GPS signal loss conditions. During the 'GPS on' periods, our system performs navigation based on the integration of GPS/INS over a filter that creates the necessary corrections for good performance. Meanwhile, the generated navigation data are used to learn the experience of the integrated navigation system. When the GPS is off, we use the previously learnt pattern to generate and supply the estimated position difference data to the INS using the same filter. This approach effectively prevents the drift of vehicle out of its path. We prove that our approach decreases the uncertainty in the navigation system caused by GPS signal loss and helps to achieve efficient navigation with the use of the low cost sensors.

Section 2 introduces the general system architecture having an optimum neural network structure with an efficient learning algorithm and Section 3 outlines the design of the neural network. The resulting system performance is analysed with examples in Section 4 and the paper concludes in Section 5.

2. ARTIFICIAL NEURAL NETWORK (ANN) ENHANCED GPS/INS.

A detailed block diagram of our enhanced GPS/INS + ANN system for the training phase with integrated GPS/INS navigation system running is shown in Figure 1, whilst the prediction phase, used when the GPS signal is lost, is shown in Figure 2.

https://doi.org/10.1017/S037346330400267X Published online by Cambridge University Press

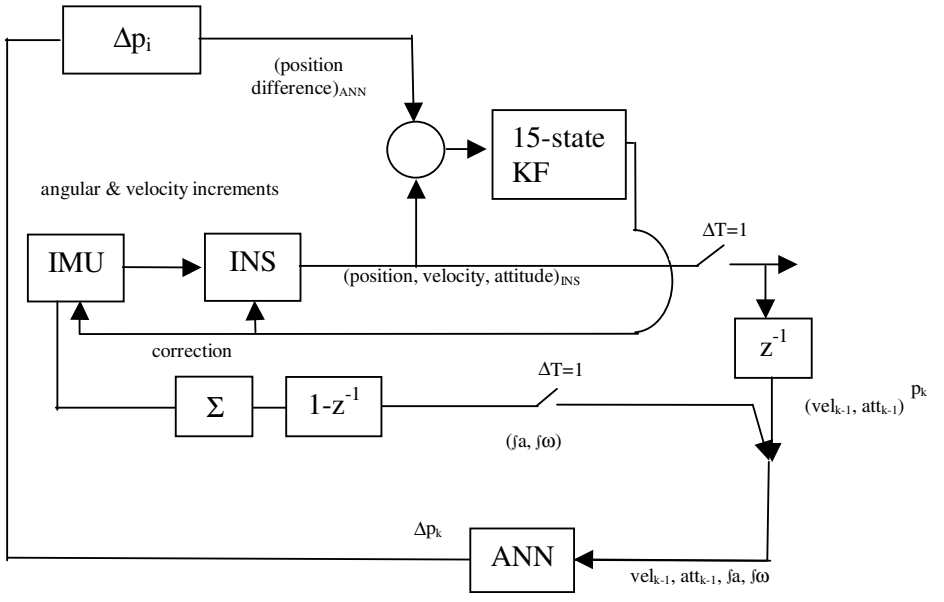

Figure 2. System block diagram with Δp aiding (prediction phase).

2.1. *Basic navigation system architecture* (*GPS*/*INS*).

2.1.1. *The inertial measurement unit*. The inertial measurement unit (IMU) uses a LITEF B-290 triad of silicon accelerometers and three LITEF μFORS-6 fibre optic gyros mounted orthogonally inside a cubical case to measure the specific force and rotation of the body with respect to the inertial frame. The gyros have bias values of 6°/hr and a scale factor of 2000 ppm, while the accelerometer biases are around 10 mg and scale factors are 3000 ppm. The accelerometer and gyroscopes provide temperature compensated data to the IMU processing card. Inertial sensor data are calibrated for scale factor, bias and misalignment. IMU data are sampled at 100 Hz for the land vehicle test where the sampling rate is directly related to the highest dynamic frequency in the vehicle. The sampled data are then sent to the navigation computer in order to generate the navigation output.

2.1.2. *GPS and INS integration*. GPS generates position and velocity outputs every second with a bounded errors of less than 15 m for position and 0·05 m/s for velocity in the land vehicle (LV) tests. The Kalman update is triggered at every GPS measurement (1 Hz) using the difference between GPS and INS solutions as the input. Hence, the Kalman filter (KF) generates the corrections for diminishing the INS and IMU errors and the overall GPS/INS output has thus a bounded uncertainty.

The navigation system implemented works in local level mechanization such that it calculates attitude and body velocity with respect to North-East-Down (NED) frame. In this type of mechanization, the rate of change of the vehicle speed with respect to earth is expressed as:

$$\frac{d}{dt}\mathbf{v}_e|_n = \frac{d}{dt}\mathbf{v}_e|_i - (\omega_{ie} + \omega_{en}) x \mathbf{v}_e \tag{1}$$

https://doi.org/10.1017/S037346330400267X Published online by Cambridge University Press

where ω_{ie} is the earth rotation rate with respect to the inertial frame and ω_{en} is the rate of the navigation frame with respect to the earth.

Substuting $\dot{\mathbf{v}}_e^i = \mathbf{f} - \omega_{ie} x \mathbf{v}_e + \mathbf{g}$ into (1), we have

$$\frac{d}{dt}\mathbf{v}_e|_n = \mathbf{f} - (2\omega_{ie} + \omega_{en}) x \mathbf{v}_e + \mathbf{g} \tag{2}$$

where $\mathbf{f}$ is the specific force and $\mathbf{g}$ is the gravity vector.

Expressing (2) in the navigation frame:

$$\dot{\mathbf{v}}_e^n = \mathbf{C}_b^n \mathbf{f}^b - (2\omega_{ie}^n + \omega_{en}^n) x \mathbf{v}_e^n + \mathbf{g}^n \tag{3}$$

Using the direction cosine matrix (DCM) method, the transformation matrix between the navigation and body frames propagates as

$$\dot{\mathbf{C}}_b^n = \mathbf{C}_b^n \Omega_{nb}^b \tag{4}$$

where Ω_{nb}^b is the skew symmetric matrix representation of the body angular speed ω_{nb}^b, with respect to the navigation frame expressed in body frame, and

$$\omega_{nb}^b = \omega_{ib}^b - \mathbf{C}_n^b(\omega_{ie}^n + \omega_{en}^n) \tag{5}$$

Using these equations, the INS computes the navigation output at a rate of 100 Hz for the land vehicle included as an example in this paper. The GPS supplies position and velocity data at 1 Hz rate computed using the satellite position and time data coming from the satellites (SVs).

One can benefit from the bounded error characteristics of the GPS and high frequency characteristics of the INS at the same time by integrating them via a Kalman filter. In the current application a 15-state Kalman filter is designed in order to integrate INS and GPS systems. The filter uses a perturbation error model which can be expressed in vector form as:

$$\begin{aligned}
&\dot{\varepsilon} = -\omega_{in}^n x \varepsilon + \delta\omega_{in}^n - \mathbf{C}_b^n \delta\omega_{ib}^b \\
&\delta\dot{\mathbf{v}}^n = \mathbf{C}_b^n \delta\mathbf{f}^b + \mathbf{C}_b^n \delta\mathbf{f}^b \times \varepsilon - (2\omega_{ie}^n + \omega_{en}^n) \times \delta\mathbf{v}^n - (2\delta\omega_{ie}^n + \delta\omega_{en}^n) \times \mathbf{v}^n + \delta\mathbf{g}^n \\
&\delta\dot{L} = \delta v_n, \delta\dot{\lambda} = \delta v_e, \delta\dot{h} = -v_d
\end{aligned} \tag{6}$$

where ε is tilt angle vector, $\delta\mathbf{v}^n$ the velocity error in navigation frame, $\delta\dot{L}$, $\delta\dot{\lambda}$ and $\delta\dot{h}$ the north, east and height position errors, respectively. In addition to these 9 error states standing for inertial equation errors, another 6 states are used in order to model the accelerometer and gyro bias errors, as a first-order Markov process:

$$\delta\dot{f}^b = -\frac{1}{\tau_a}\delta f^b + w, \delta\dot{\omega} = -\frac{1}{\tau_g}\delta\omega + w \tag{7}$$

where w is white noise. Based on experimental observations of the inertial sensors, the Markov process time constants, τ_a and τ_g, are set to 360 seconds. Using the differential equations given, one can create the continuous state transition matrix, F, for the error states, which is then discretised for the Kalman filter using the first order Taylor series approximation to yield, $\Phi = \mathbf{I} + \mathbf{F}\Delta t$ where Δt is chosen as 0·5 seconds and Kalman propagation of the covariance

$$\mathbf{P}^- = \Phi\mathbf{P}^+\Phi^T + \mathbf{Q} \tag{8}$$

https://doi.org/10.1017/S037346330400267X Published online by Cambridge University Press

is done at 2 Hz for our application. At this stage, there is no state propagation since the state is fed back into the integrated system at every update time in order to correct the inertial system and sensor errors.

The Kalman update is triggered at every GPS measurement (1 Hz) using:

$$\begin{aligned} \mathbf{K} &= \mathbf{P}^{-}\mathbf{H}^{T}(\mathbf{H}\mathbf{P}^{-}\mathbf{H}^{T}+\mathbf{R})^{-1} \\ \delta\mathbf{x} &= \mathbf{K}\mathbf{y} \\ \mathbf{P}^{+} &= (\mathbf{I}-\mathbf{K}\mathbf{H})\mathbf{P}^{-} \end{aligned} \tag{9}$$

where $\delta\mathbf{x}$ is the estimated error states, $\mathbf{y}$ the difference between GPS measurements (position and velocity) and INS measurements, $\mathbf{K}$ the Kalman gain matrix, $\mathbf{P}$ the state covariance matrix, $\mathbf{R}$ the measurement covariance matrix, $\mathbf{Q}$ the input covariance matrix and $\mathbf{H}$ the measurement matrix: $\mathbf{H}=[\mathbf{I}_{6\times 6} \quad \mathbf{0}_{6\times 9}]$ where the position and velocity errors are observed. $\mathbf{R}$ matrix is a constant matrix. $\mathbf{R}=diag\,([15 \quad 15 \quad 15 \quad 0{\cdot}1 \quad 0{\cdot}1 \quad 0{\cdot}1]^2)$ is chosen based on the GPS output uncertainties. At initial $\mathbf{P}$, the diagonal matrix has diagonal entities of state variances, standard deviations of position, velocity and attitude as 5 m, 0·1 m/s and 1 mrad, respectively. The standard deviations of the accelerometers are taken as 10 mg and 6°/hr. The $\mathbf{Q}$ matrix is created using the bias values.

2.1.3. *GPS and INS general performance.*

2.1.3.1. *Test setup.* The basic integrated navigation system is mounted on a van and tested on a 10-minute route. The vehicle contains the inertial navigation system, power system, GPS and two computers. A laptop computer is used to store GPS and IMU data and a desktop computer is employed for system health monitoring. The vehicle began the test from a standing start and experienced velocities exceeding 70 km/h. The hardware contains a GPS/INS integrated navigation system employing a tactical grade IMU, navigation computer and a GPS receiver. The IMU contains three 6°/hr gyroscopes and one 10 mg three-axis accelerometer in an orthogonal arrangement. A GPS/INS system containing a TMS320C31 microprocessor for navigation computation and a Novatel 3151R OEM receiver is mounted on the test vehicle for navigation purposes.

The test system also contains two computers. A laptop computer is employed for data collection purposes. Raw IMU data was logged at 100 Hz while the GPS data was logged at 1 Hz. Both GPS and IMU data were stored through a serial port on the laptop computer. During the test, GPS/INS navigation solutions were also recorded to analyse the performance of the integrated navigation system. The desktop computer is used to monitor real time navigation solutions and the health status of the overall system.

The land vehicle test was carried out in the campus of Middle East Technical University populated with trees and the buildings and an open field with minimal buildings and no trees around. A 600 second test was conducted on the campus site. The campus site test trajectory is shown in Figure 3. The campus path circles around a 1500 m × 400 m area and generates a closed path of nearly 5 kilometres long.

2.1.3.2. *Performance analysis.* During the vehicle test the GPS position, velocity, heading, INS position, velocity, attitude and GPS/INS position, velocity and attitude data are recorded for 600 seconds. Figure 4a shows the GPS/INS and INS-only horizontal position solutions. As seen in the figure, the INS-only solution wanders out of the scope due to the sensor errors at the first 100 second of the 600-second test.

https://doi.org/10.1017/S037346330400267X Published online by Cambridge University Press

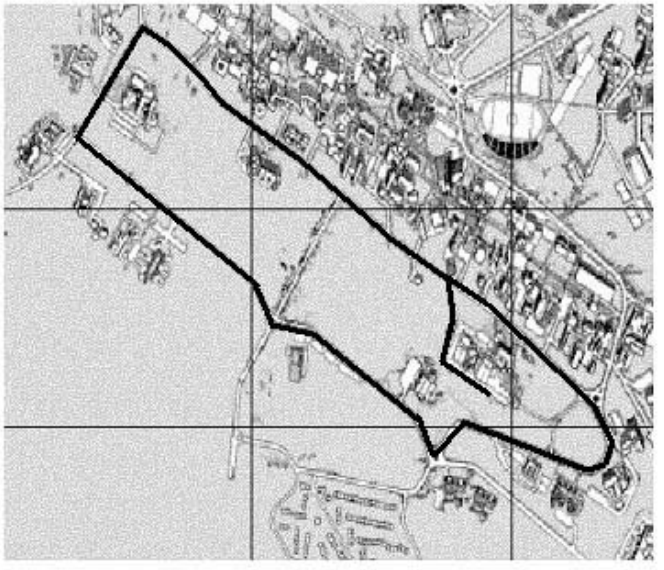

Figure 3. The campus site test trajectory.

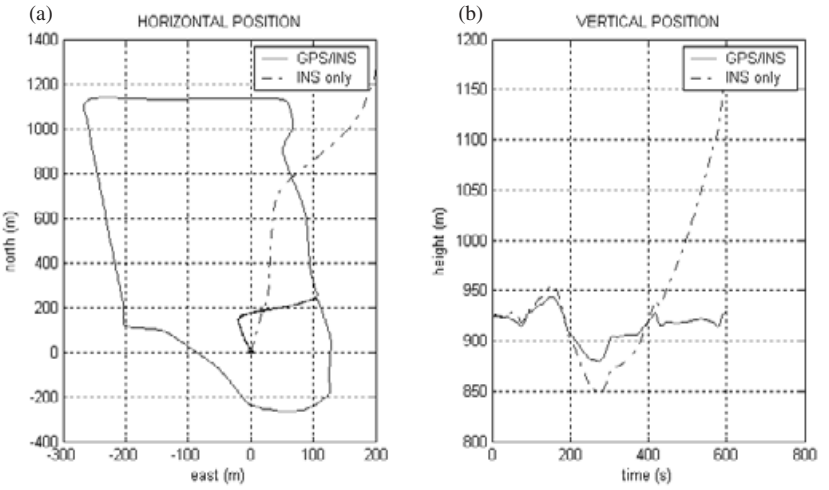

Figure 4. (a) Horizontal navigation using INS only and using integrated INS/GPS. (b) Vertical profile of the test route output by GPS/INS and by INS only.

Figure 4b presents the vertical positions provided by the inertial and the integrated systems. During the test the inertial system alone gives the position estimation with an error again drifting away into very high values. The GPS/INS system on the other hand has an uncertainty in the position estimation that is not more than a few metres. However, when GPS turns off for a long period of time, leaving the INS alone, the

https://doi.org/10.1017/S037346330400267X Published online by Cambridge University Press

initial alignment errors of INS propagate with an uncertainty that grows with time. Bounding off INS errors during GPS signal loss is the motivation of Section 2.2 and will be investigated thoroughly in the following sections.

2.2. *GPS/INS enhanced by an intelligent architecture, the ANN*. The enhancement provided to the GPS/INS integration through an intelligent architecture operates in two different phases:

- learning the behaviour as GPS signals integrated to the navigation (training phase),
- acting as an intelligent compensator in case of GPS signal losses (prediction phase).

2.2.1. *Training phase*. The block diagram of GPS/INS + ANN in training phase is shown in Figure 1. In this figure, the position difference $\Delta\mathbf{p}_k$ which is a three dimensional vector with north position, east position and height as components, is a function of velocity $\mathbf{v}$ and attitude ϕ states of the navigation system and the integral of acceleration ($\mathbf{a}$) and rotation rates ($\boldsymbol{\omega}$) which appears as the summation of angle and velocity increments:

$$\Delta\mathbf{p}_k = \begin{bmatrix} \Delta L \\ \Delta\lambda \\ \Delta h \end{bmatrix} = \mathbf{p}_k - \mathbf{p}_{k-1} = f\left(\mathbf{v}_{k-1}, \Phi_{k-1}, \int_{t_{k-1}}^{t_k} \mathbf{a}, \int_{t_{k-1}}^{t_k} \boldsymbol{\omega}\right) \tag{10}$$

The GPS/INS states given in (10) are the inputs to the ANN of the navigation system. After every update triggered by GPS measurements, the database created for ANN training phase records the previous updated states of GPS/INS (velocity and attitude) and summation of IMU velocity and angle increments of the last second as input. The position difference between the current and the previous position, $\Delta\mathbf{p}_k$ is recorded as the output until the loss of GPS signal. During the training phase, the forward and backward computations are iteratively repeated by injecting recorded data recursively to the network until the performance criteria are met.

2.2.2. *Prediction phase*. Whenever the GPS signal is absent, ANN leaves its training phase and estimates every second the position difference, $\Delta\mathbf{p}_k$. This calculated position difference is then used in the place of the non-existing GPS position as input to the Kalman filter (Figure 2). Our approach helps the system to drift much more slowly than the classical GPS/INS integration and its performance is demonstrated in Section 4.

3. ARTIFICIAL NEURAL NETWORK (ANN) DESIGN.

The ANN is a multilayer perceptron (MLP)-based intelligent structure and is composed of three main layers. These are the pre-processing, neural networks layers and post-processing layers. The internal structure of the system is shown in Figure 5.

The neural network is made more efficient, reliable and stable when pre-processing is applied on the network inputs. ANN inputs are scaled so as to normalize the mean and standard deviation of the training set in a manner that shift them to zero mean and unity standard deviation.

https://doi.org/10.1017/S037346330400267X Published online by Cambridge University Press

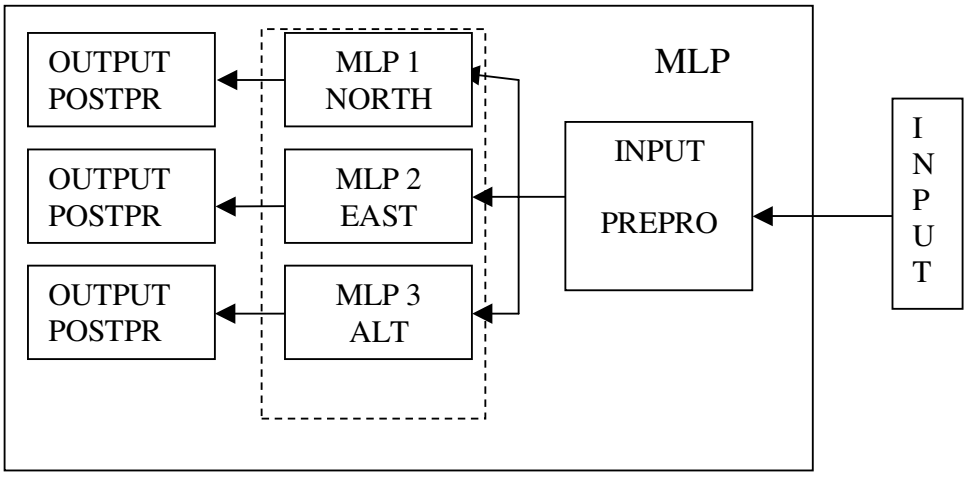

Figure 5. MLP based intelligent estimator.

The second layer of the structure is composed of three separate multilayer perceptrons, each of which predicts the position differences in orthogonal directions. Instead of having a single architecture that outputs a vector of direction estimates, the three-MLP architecture is used to avoid coupled learning during training where degradation of one output may occur while the others improve. This approach also increases the speed of convergence of the overall system by decreasing the number of neurons in each MLP because, instead of one MLP with three outputs and a high number of hidden layer neurons, the proposed structure exploits three MLPs with relatively low numbers of neurons.

The MLP outputs are sent to the last layer of for post-processing where they are rescaled in the same manner as pre-processing. This scaling is also applied to the outputs that are generated by the network in the prediction phase.

3.1. *Training algorithm*. A critical and effective issue determining ANN efficiency is the learning algorithm of the training phase as shown in Haykin, 1997; Cichocki and Unbehauen, 1992; Simpson, 1990. There are various learning algorithms with different efficiency and computational load. The difficulty in choosing one for a defined problem stems from fact that one algorithm is not optimum for every single problem. In order to determine the most effective algorithm for GPS/INS enhancement, we ran a through comparative analysis based on the results of different algorithms. The back-propagation algorithms compared were:

- gradient descent with adaptive step size,
- conjugate gradient,
- Levenberg-Marquardt (LM).

The results of the comparison are given in Section 3.3.

3.2. *Neural network topology*. The artificial neural network based on the multilayer perceptron is a feedforward network with one or more layers between its input and output layers acting as a universal approximator. The number of layers and the number of nodes existing in each layer depends mainly on the complexity of the target function. If an insufficient number of neurons is assigned to each layer, the neural

https://doi.org/10.1017/S037346330400267X Published online by Cambridge University Press

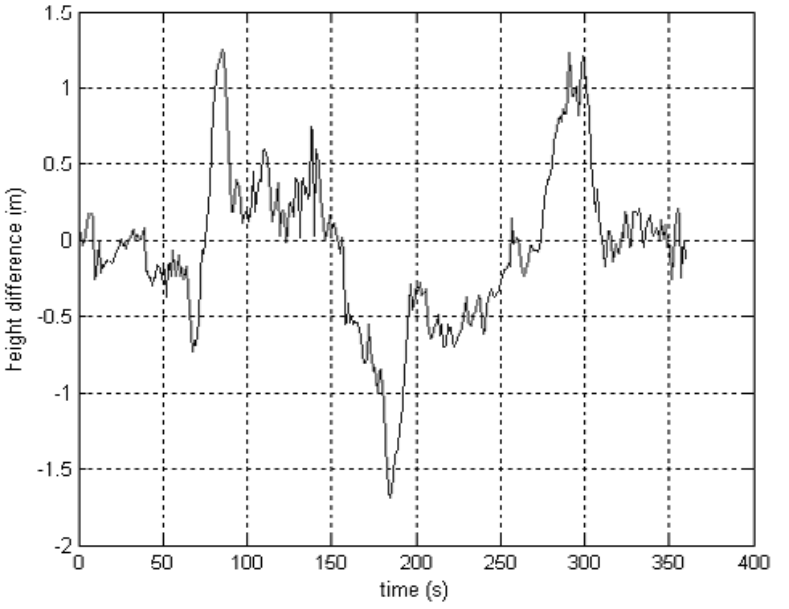

Figure 6. The height difference data employed as ANN output in order to compare different training algorithms and ANN topologies.

network may fail to express the input/output relationship accurately. On the other hand, a neural network with an excessive number of neurons may show instability and tend to memorize the training set instead of learning the input/output relation. The topology study conducted seeks an optimum number of hidden layers and optimum number of neurons in each layer. The details and results of this study are given in Section 3.3.

3.3. *Optimum neural network structure*. The candidate neural networks and training algorithms were compared with the input data set composed of the first 360 seconds of the land test given in Section 2, and the desired output is the height difference given in Figure 6 without loss of generality. Moreover, each candidate network was run to estimate the height for the remaining 240 seconds of the test and the resulting height errors compared in order to choose the optimum topology and training algorithm. The structure selected for height estimation was also accepted to be optimum for north and east position networks without loss of generality.

The candidate networks were run in the training phase with different training algorithms until their convergence rates fell below $2{\cdot}5 \times 10^{-2}$; their resulting performance characteristics are given as the run time (with Pentium IV-2.0 GHz) and root mean square error in Table 1. Each network was run five times in order to eliminate the random effects stemming from network initialisation and the mean of five runs are given in the table.

As seen in the table, based on the efficiency in mean square error and time of convergence, the $12 \times 6 \times 3 \times 1$ topology trained by the Levenberg-Marquardt learning algorithm is the most reliable structure. Consequently, the $12 \times 6 \times 3 \times 1$ topology

https://doi.org/10.1017/S037346330400267X Published online by Cambridge University Press

Table 1. Comparison of different neural network architectures.

Topology	Transfer functions	Algorithm	Time (s)	RMS (cm)
$12\times3\times1$	tansig-linear	gd with adaptive step size	1·797	8·26
$12\times3\times1$	tansig-linear	Conjugate gradient	0·577	8·27
$12\times3\times1$	tansig-linear	Levenberg-Marquardt	0·248	8·23
$12\times6\times1$	tansig-linear	gd with adaptive step size	1·630	5·36
$12\times6\times1$	tansig-linear	Conjugate gradient	0·523	5·41
$12\times6\times1$	tansig-linear	Levenberg-Marquardt	0·225	5·33
$12\times9\times1$	tansig-linear	gd with adaptive step size	1·911	5·17
$12\times9\times1$	tansig-linear	Conjugate gradient	0·615	5·19
$12\times9\times1$	tansig-linear	Levenberg-Marquardt	0·265	5·14
$12\times6\times3\times1$	logsig-tansig-linear	gd with adaptive step size	1·768	5·44
$12\times6\times3\times1$	logsig-tansig-linear	Conjugate gradient	0·567	5·53
$12\times6\times3\times1$	logsig-tansig-linear	Levenberg-Marquardt	0·244	5·41
$12\times6\times6\times1$	logsig-tansig-linear	gd with adaptive step size	2·543	3·78
$12\times6\times6\times1$	logsig-tansig-linear	Conjugate gradient	0·761	3·87
$12\times6\times6\times1$	logsig-tansig-linear	Levenberg-Marquardt	0·646	3·63
$12\times6\times9\times1$	logsig-tansig-linear	gd with adaptive step size	3·675	2·91
$12\times6\times9\times1$	logsig-tansig-linear	Conjugate gradient	1·108	3·01
$12\times6\times9\times1$	logsig-tansig-linear	Levenberg-Marquardt	0·917	2·74

with Levenberg-Marquardt learning algorithm was implemented for the ANN enhancement of the GPS/INS integration. The height error results for each topology trained with LM algorithm are also given in Figure 7.

3.4. *ANN predicted position difference aiding to GPS/INS.* During GPS signal loss periods, the intelligent navigation system architecture provides ANN based prediction of position differences that are input to the Kalman filter for an intelligent information support. These inputs are the position difference estimates from the ANN and INS calculated position differences. Within the Kalman algorithm, these error inputs should be related to the filter states through an observation matrix.

These measurement residuals formed by differencing ANN and INS solutions are

$$\mathbf{z}_k = \delta\Delta\mathbf{p}_k = \Delta\mathbf{p}_{I,k} - \Delta\mathbf{p}_{N,k} = \mathbf{p}_{I,k} - \mathbf{p}_{I,k-1} - (\mathbf{p}_{N,k} - \mathbf{p}_{N,k-1}) + \mathbf{w}_k \tag{11}$$

where I stands for INS, N stands for ANN, and $\mathbf{w}_k$ is the noise on ANN predictions. (11) may be rearranged as

$$\mathbf{z}_k = \delta\Delta\mathbf{p}_k = \mathbf{p}_{I,k} - \mathbf{p}_{N,k} - (\mathbf{p}_{I,k-1} - \mathbf{p}_{N,k-1}) + \mathbf{w}_k = \delta\mathbf{p}_k - \delta\mathbf{p}_{k-1} + \mathbf{w}_k \tag{12}$$

and

$$\delta\mathbf{p}_{k-1} = \delta\mathbf{p}_k - \Delta t\delta\mathbf{v}_k^n + \tfrac{1}{2}\Delta t^2\mathbf{C}_b^n\delta\mathbf{f}_k^b \tag{13}$$

Thus, substituting (13) into (12) and taking measurement interval $\Delta t = 1$ second, the Kalman measurement is expressed as

$$\mathbf{z}_k = \delta\Delta\mathbf{p}_k = \delta\mathbf{v}_k^n - \tfrac{1}{2}\mathbf{C}_b^n\delta\mathbf{f}_b^k + \mathbf{w}_k \tag{14}$$

https://doi.org/10.1017/S037346330400267X Published online by Cambridge University Press

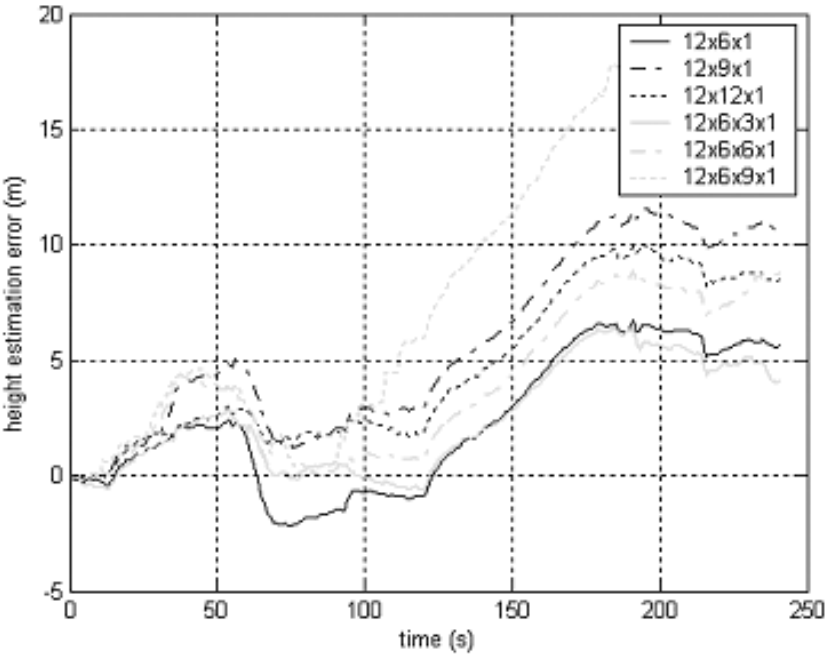

Figure 7. Performance of candidate ANN networks trained by Levenberg-Marquardt algorithm.

Exploiting (14), the Kalman measurement matrix H takes the following form

$$\mathbf{H} = [\,\mathbf{0}_{3\times 3} \quad \mathbf{I}_{3\times 3} \quad \mathbf{0}_{3\times 3} \quad -\tfrac{1}{2}\mathbf{C}_b^n \quad \mathbf{0}_{3x3}\,] \tag{15}$$

where the 15-state Kalman filter state vector is

$$[\delta L \quad \delta\lambda \quad \delta h \quad \delta v_n \quad \delta v_e \quad \delta v_d \quad \varepsilon_x \quad \varepsilon_y \quad \varepsilon_z \quad \delta f_x \quad \delta f_y \quad \delta f_z \quad \delta\omega_x \quad \delta\omega_y \quad \delta\omega_z]^T \tag{16}$$

Modelling the uncertainty in measurement noise covariance matrix as 10 times of the training values of $\sigma_{h,n,e} \cong 0{\cdot}15$ m, $\mathbf{R}_{3\times 3}$ may be expressed as

$$\mathrm{R} = 2.25\mathbf{I}_{3\times 3} \tag{17}$$

4. EXPERIMENTAL RESULTS.

4.1. *Test set-up.* The land vehicle set-up employed in the ANN enhanced integrated navigation system is exactly the same as the one given in Section 2.1.3.1. This test was conducted again in Middle East Technical University campus for 500 seconds and raw IMU data, GPS data and GPS/INS data were collected throughout the test. INS-only data and ANN aided navigation data was obtained by post-processing of the raw IMU data. ANN was trained using the test data collected

https://doi.org/10.1017/S037346330400267X Published online by Cambridge University Press

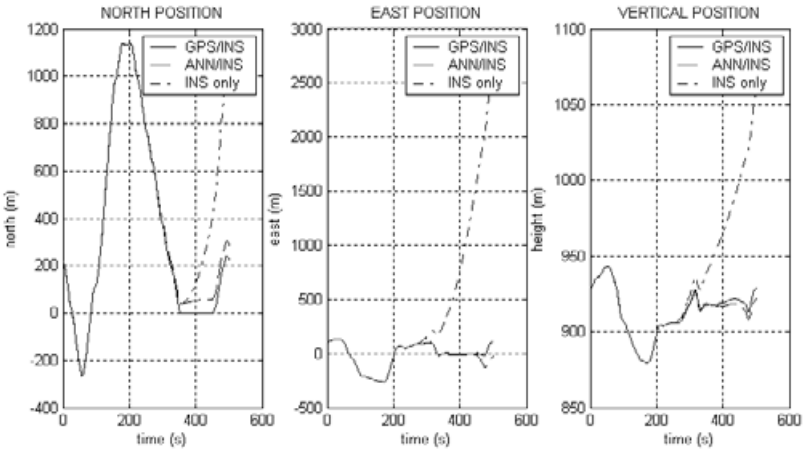

Figure 8. (a) North (b) East (c) Height solution.

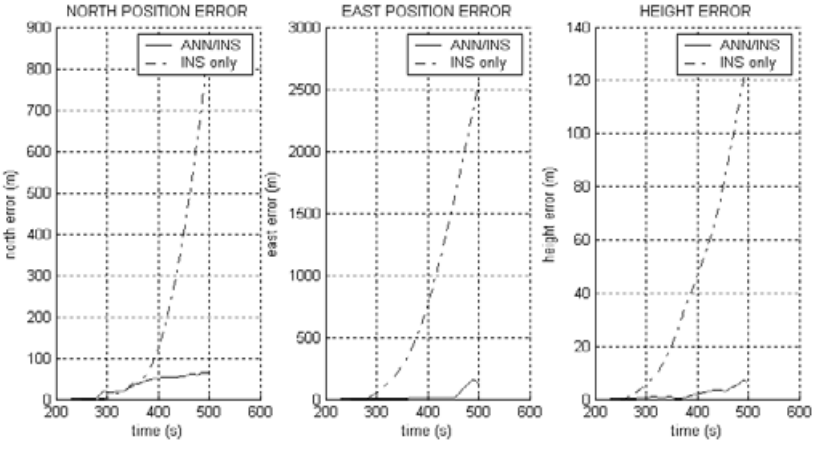

Figure 9. (a) North (b) East (c) Height error.

within the first 230 seconds of the route in which the GPS signal was available; afterwards it estimates the position difference for the remaining 270 seconds of the test when the GPS/INS system behaves as INS-only because of GPS signal loss.

4.2. *Test results.* In this section the GPS/INS computed navigation solution is employed as reference and the intelligent navigation system and inertial system is compared to this reference in order to determine the performances. Figure 8 presents the north position, east position and height solutions of GPS/INS, INS-only and ANN/INS structures. The position errors of INS-only, and ANN/INS systems are given in Figure 9. It is seen from the figures that both of the ANN aided intelligent navigation systems achieve the proposed suppression of the INS-only structure errors. The ANN aided systems height solutions are within a few metres throughout the navigation due to the fact that ANN training set in this channel covers more

https://doi.org/10.1017/S037346330400267X Published online by Cambridge University Press

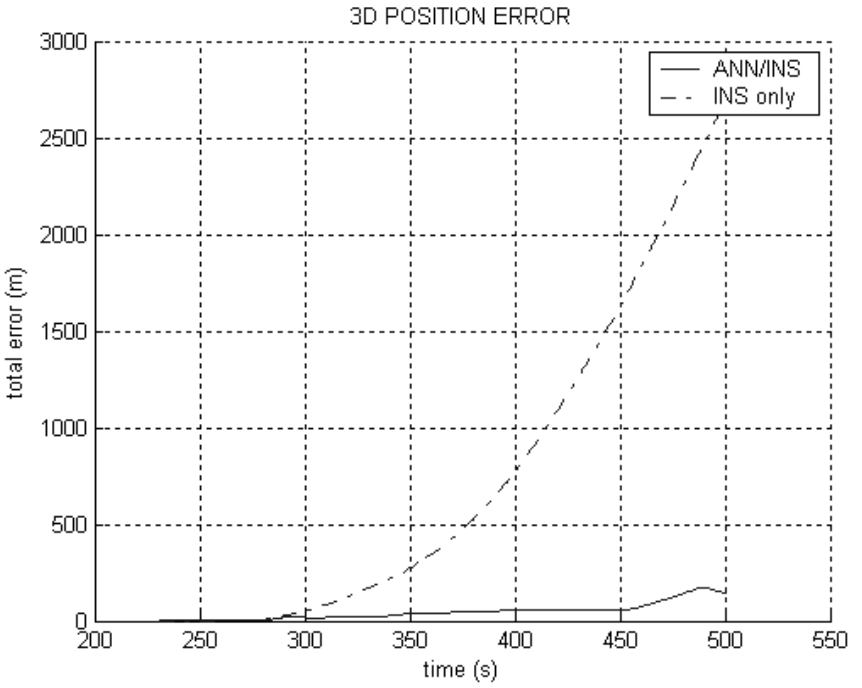

Figure 10. 3-dimensional position error during 270 seconds of GPS loss.

information than the other channels. Both sets of Figures show that ANN/INS provides the better navigation solutions during the GPS loss period. This structure forces the errors down to zero for a long time and presents high performance. The proposed system shows that with enough training, it can decrease a 3 km error to 200 metres (Figure 10). It provides accurate position solutions beyond a GPS signal loss of 270 seconds.

5. CONCLUSION. The GPS/INS system provides very accurate, reliable and robust navigation results. GPS aiding to correct position, velocity, attitude, accelerometer bias and gyroscope drift yields accurate navigation data. The INS-only system is insufficiently accurate for navigation purposes during the test runs. Therefore, an alternative structure employing the artificial neural network predictions was presented and it was shown that this approach diminished the errors and allowed the inertial system to navigate more accurately without any external aid. Comparisons showed that the proposed system provides more accurate results in the absence of GPS signal. The proposed structure is found to perform extremely well in land vehicle test since GPS/INS + ANN system learns the navigation behaviour patterns by experience when the GPS signals are available to aid to the system accuracy. The intelligent navigation system is shown to be capable of decreasing the system position error to less than 1/10th of INS-only error in the case of GPS signal loss.

https://doi.org/10.1017/S037346330400267X Published online by Cambridge University Press

REFERENCES

Brown, G.B., and Hwang, P.Y.C. (1992). *Introduction to Random Signals and Applied Kalman Filtering*. John Wiley & Sons, Inc.

Cichocki, A., and Unbehauen, R. (1992). *Neural Network for Optimization and Signal Processing*. John Wiley & Sons, Inc.

Haykin, S. (1997). *Neural Networks*. Prentice-Hall, Inc.

Kaygısız, B., Erkmen, A.M., and Erkmen, I. (2003-accepted). GPS/INS enhancement using neural networks for autonomous ground vehicle applications. *Proceedings of the IEEE/RJS International Conference on Intelligent Robots and Systems*. Las Vegas, Nevada.

Kaygısız, B., and Gökpınar, S. (2003). GPS/INS guided field artillery munitions. *Proceedings of the AFCEA*. Ankara, Turkey.

Kelly, A.J. (1994). A 3D State Space Formulation of a Navigation Kalman Filter for Autonomous Vehicles. *Technical Report of Robotics Institute-Carnegie Mellon University*.

Lewantowicz, Z.H., and Paschall, R.N. (1995). Deep integration of GPS, INS, SAR and other sensor information. *AGARD 331*-Aerospace Navigation Systems.

Simpson, P.K. (1990). *Artificial Neural Systems*. Academic Press, Inc.

Titterton, D.H., and Weston, J.L. (1997). *Strapdown Inertial Navigation Systems*. Peter Peregrinus Ltd.